



Article

PPAR β/δ Ligands Regulate Oxidative Status and Inflammatory Response in Inflamed Corpus Luteum—An In Vitro Study

Karol Mierzejewski ^{1,*}, Aleksandra Kurzyńska ¹, Zuzanna Gerwel ¹, Monika Golubska ¹, Robert Stryński ² and Iwona Bogacka ^{1,*}

¹ Department of Animal Anatomy and Physiology, Faculty of Biology and Biotechnology, University of Warmia and Mazury in Olsztyn, 10-719 Olsztyn, Poland

² Department of Biochemistry, Faculty of Biology and Biotechnology, University of Warmia and Mazury in Olsztyn, 10-719 Olsztyn, Poland

* Correspondence: karol.mierzejewski@uwm.edu.pl (K.M.); iwonab@uwm.edu.pl (I.B.);
Tel.: +48-89-523-35-93 (K.M.); +48-89-523-44-20 (I.B.)

Abstract: Inflammation in the female reproductive system causes serious health problems including infertility. The aim of this study was to determine the in vitro effects of peroxisome proliferator-activated receptor-beta/delta (PPAR β/δ) ligands on the transcriptomic profile of the lipopolysaccharide (LPS)-stimulated pig corpus luteum (CL) in the mid-luteal phase of the estrous cycle using RNA-seq technology. The CL slices were incubated in the presence of LPS or in combination with LPS and the PPAR β/δ agonist—GW0724 (1 $\mu\text{mol/L}$ or 10 $\mu\text{mol/L}$) or the antagonist—GSK3787 (25 $\mu\text{mol/L}$). We identified 117 differentially expressed genes after treatment with LPS; 102 and 97 differentially expressed genes after treatment, respectively, with the PPAR β/δ agonist at a concentration of 1 $\mu\text{mol/L}$ or 10 $\mu\text{mol/L}$, as well as 88 after the treatment with the PPAR β/δ antagonist. In addition, biochemical analyses of oxidative status were performed (total antioxidant capacity and activity of peroxidase, catalase, superoxide dismutase, and glutathione S-transferase). This study revealed that PPAR β/δ agonists regulate genes involved in the inflammatory response in a dose-dependent manner. The results indicate that the lower dose of GW0724 showed an anti-inflammatory character, while the higher dose seems to be pro-inflammatory. We propose that GW0724 should be considered for further research to alleviate chronic inflammation (at the lower dose) or to support the natural immune response against pathogens (at the higher dose) in the inflamed corpus luteum.

Keywords: corpus luteum; pig; inflammation; oxidative stress; GW0724



Citation: Mierzejewski, K.; Kurzyńska, A.; Gerwel, Z.; Golubska, M.; Stryński, R.; Bogacka, I. PPAR β/δ Ligands Regulate Oxidative Status and Inflammatory Response in Inflamed Corpus Luteum—An In Vitro Study. *Int. J. Mol. Sci.* **2023**, *24*, 4993. <https://doi.org/10.3390/ijms24054993>

Academic Editors: Walter Wahli and Manuel Vázquez-Carrera

Received: 6 January 2023

Revised: 19 February 2023

Accepted: 3 March 2023

Published: 5 March 2023



Copyright: © 2023 by the authors. Licensee MDPI, Basel, Switzerland. This article is an open access article distributed under the terms and conditions of the Creative Commons Attribution (CC BY) license (<https://creativecommons.org/licenses/by/4.0/>).

1. Introduction

Increasing infertility due to chronic inflammation has become a serious problem and a challenge for human and veterinary medicine in recent years. Inflammation is a protective response to pathological conditions such as bacterial infections. However, if the inflammatory cascade is not stopped, it transforms into chronic inflammation and leads to organ dysfunction [1]. An inflammatory response in the female reproductive system is often associated with the presence of lipopolysaccharide (LPS), the endotoxin of Gram-negative bacteria, e.g., *Escherichia coli* (*E. coli*) [2]. LPS binds to TLR and stimulates the synthesis of various pro-inflammatory cytokines such as IL-1 β , IL-6, IL-8 and TNF- α [3].

There is evidence that *E. coli* LPS causes infertility by interfering with ovarian follicular development and the ovulation process [4]. Luttgenu et al. [5] reported that luteal TLR2 and TLR4 appear to be involved in the immune response of the corpus luteum (CL), which may be related to the production of pro-inflammatory cytokines and decreased ovarian steroidogenesis in cows. LPS has been reported to alter ovarian axis hormone secretion by affecting GnRH and LH production, CL growth and functions, the timing of ovulation and the estrous cycle [6,7]. In addition, the treatment of cows with LPS altered the structure of the CL and decreased plasma progesterone levels (P₄), resulting in a temporary suppression

of luteal function [8]. Despite these reports, there is a lack of data on the effect of LPS on the functions of the porcine CL. Furthermore, the great anatomical and physiological similarity of the female and porcine reproductive systems and the course of bacterial infection makes the pig a good model for studying the in vitro effects of infection on the immune response in the CL [9].

Peroxisome proliferator-activated receptors (PPARs) are ligand-dependent transcription factors belonging to the nuclear receptor superfamily. To date, three isoforms of PPARs— α , β/δ and γ —have been described [10]. PPARs have been reported to be involved in the various processes necessary for the proper functioning of the ovaries, such as the regulation of steroidogenesis, angiogenesis, tissue remodeling, cell cycle and apoptosis [11]. There is evidence that PPAR γ ligands may play a luteotropic role by increasing the activity of 3 β -HSD and the secretion of progesterone [12,13]. However, there is limited information on the role of PPAR β/δ ligands in CL function. The anti-inflammatory effects of PPAR ligands have been widely reported, including in our previous work, but most of this relates to the PPAR γ isoform [14–16]. The effect of PPAR β/δ on inflammation has not been fully elucidated [17]. In some cases, PPAR β/δ agonists appear to exert anti-inflammatory effects, such as inhibiting the synthesis of pro-inflammatory cytokines TNF- α and MCP-1 in the liver, alleviating inflammation in experimental autoimmune encephalomyelitis, or inhibiting diabetic nephropathy by reducing inflammatory mediators in mice [18–20]. There are also reports suggesting that PPAR β/δ signaling promotes inflammation [17]. It has been reported that in mice with arthritis, mesenchymal stem cells (MSCs) had higher anti-inflammatory potential than the MSCs derived from PPAR β/δ knockout mice [21].

The present study was conducted to determine the influence of PPAR β/δ ligands on the global transcriptomic profile of the LPS-stimulated corpus luteum of pigs during the mid-luteal phase of the estrous cycle. In addition, transcriptomic changes in the CL after the treatment with LPS alone have been described. For the first time, our research has revealed the role of PPAR β/δ in the regulation of oxidative stress and genes involved in the inflammatory response. In addition, we have shown a dose-dependent effect of the tested agonists.

2. Results

2.1. Statistics of RNA Sequencing

RNA sequencing data were created for 20 cDNA libraries, including four untreated samples (controls), four with LPS, four with GW0724 at a concentration of 1 μ mol/L, four with GW0724 at a concentration of 10 μ mol/L and four with GSK3787. The analysis produced 968,505,414 raw paired-end reads in total, with an average 48,425,271 per sample and a Q20 value that was on average 99.94%. The short reads, low-quality sequences and ambiguous nucleotides were removed from the raw reads, leaving on average of 938,720,608 valid reads per sample, that were used for further analysis (Supplemental Table S2). The filtered reads were mapped to the Ss11.1.98 version of the pig genome with a unique mapped average rate of 94%. The analysis of the distribution of mapped reads to gene structures indicated that 94.11% of read pairs (in average per sample) mapped to coding sequences, 3.56% mapped to introns, and 2.33% mapped to intergenic regions (Figure 1). RNA-seq data have been deposited in the ArrayExpress database at EMBL-EBI under accession number E-MTAB-12027.

2.2. The Effect of LPS on Differential Gene Expression in the Corpus Luteum

The RNA-Seq analysis revealed 117 DEGs (63 downregulated and 54 upregulated) in porcine CL on days 10–12 after LPS treatment (Figures 2A and 3A). The Gene Ontology (GO) analysis assigned these DEGs to 159 terms of biological processes, 18 terms of cellular components, and 47 terms of molecular functions (Figure 4A). The treatment of the CL tissue with LPS altered the expression of genes involved in processes such as the regulation of signaling receptor activity (*INSL6*, *IL-6*, *TNFSF14*, *IFN-DELTA-7*, *PDYN*, *PRL*), response to

bacterium (*C15orf48*, *NLRP6*, *ENSSSCG00000037358*) or oxidoreductase activity (*ALOX12B*, *ALDH3B2*, *XDH*, *SOD2*). Moreover, KEEG enrichment analysis revealed that DEGs were involved in signaling pathways such as cytokine–cytokine receptor interaction (*TNFRSF9*, *IL-6*, *TNFSF14*, *IL-27*, *PRL*) or the NOD-like receptor signaling pathway (*NLRP6*, *IL-6*, *ENSSSCG0000007964*) (Supplemental Figure S1A). All detailed DEGs, GO and KEEG results were described in Supplemental Tables S3–S5, respectively.

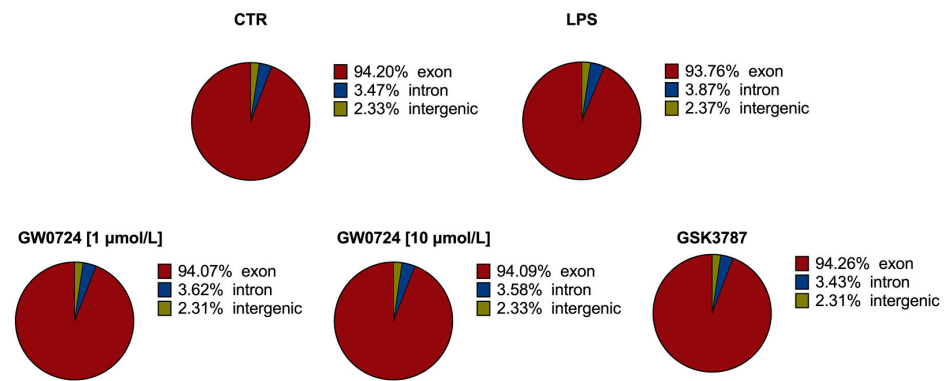


Figure 1. Distribution of mapped reads to genes structures.

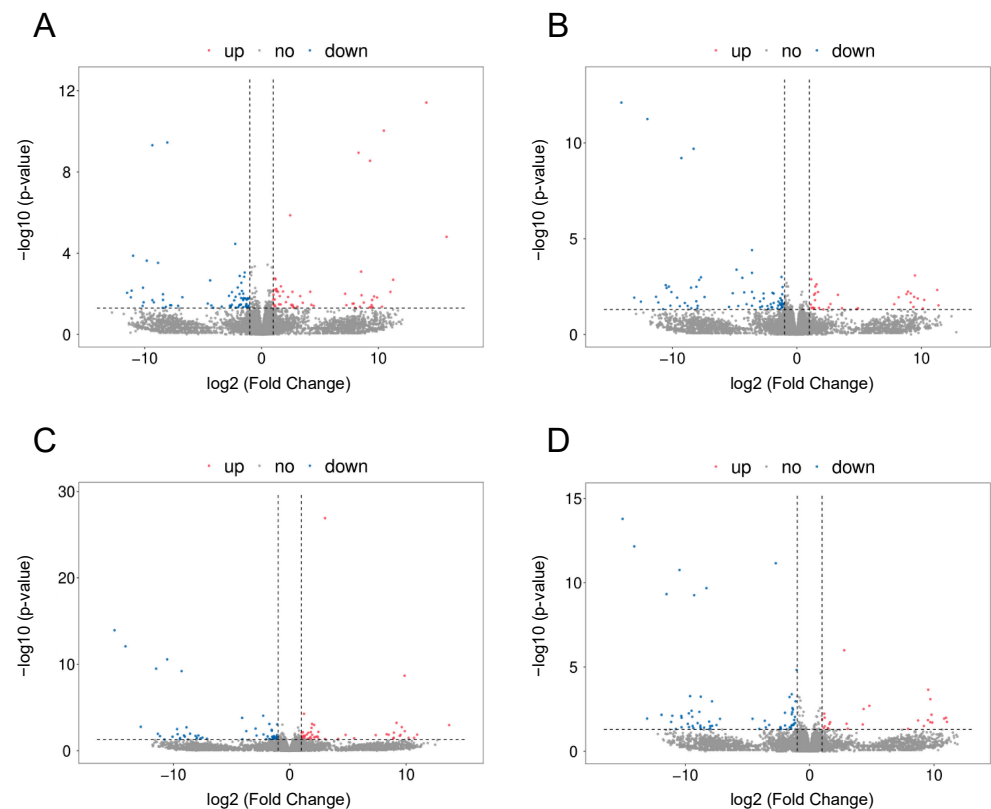


Figure 2. Volcano plots describing the abundance of transcript expression profiles after LPS (A); or LPS in combination with: GW0724 at a concentration of 1 µmol/L (B), GW0724 at a concentration of 10 µmol/L (C), and GSK3787 (D) treatment in mid-luteal phase in the corpus luteum. Logarithmic fold changes in expression (\log_2FC) are plotted on the x-axis against normalized adjusted p -values (y-axis). The sharp horizontal line denotes the negative logarithmic adjusted p -value (0.05) cut-off. Sharp vertical lines denote the fold change cut-off (absolute value of $\log_2FC > 1$). Points represent gene expression values, where blue (underexpressed) and red (overexpressed) points denote significant genes (adjusted p -value < 0.05). Grey dots indicate non-significant genes.

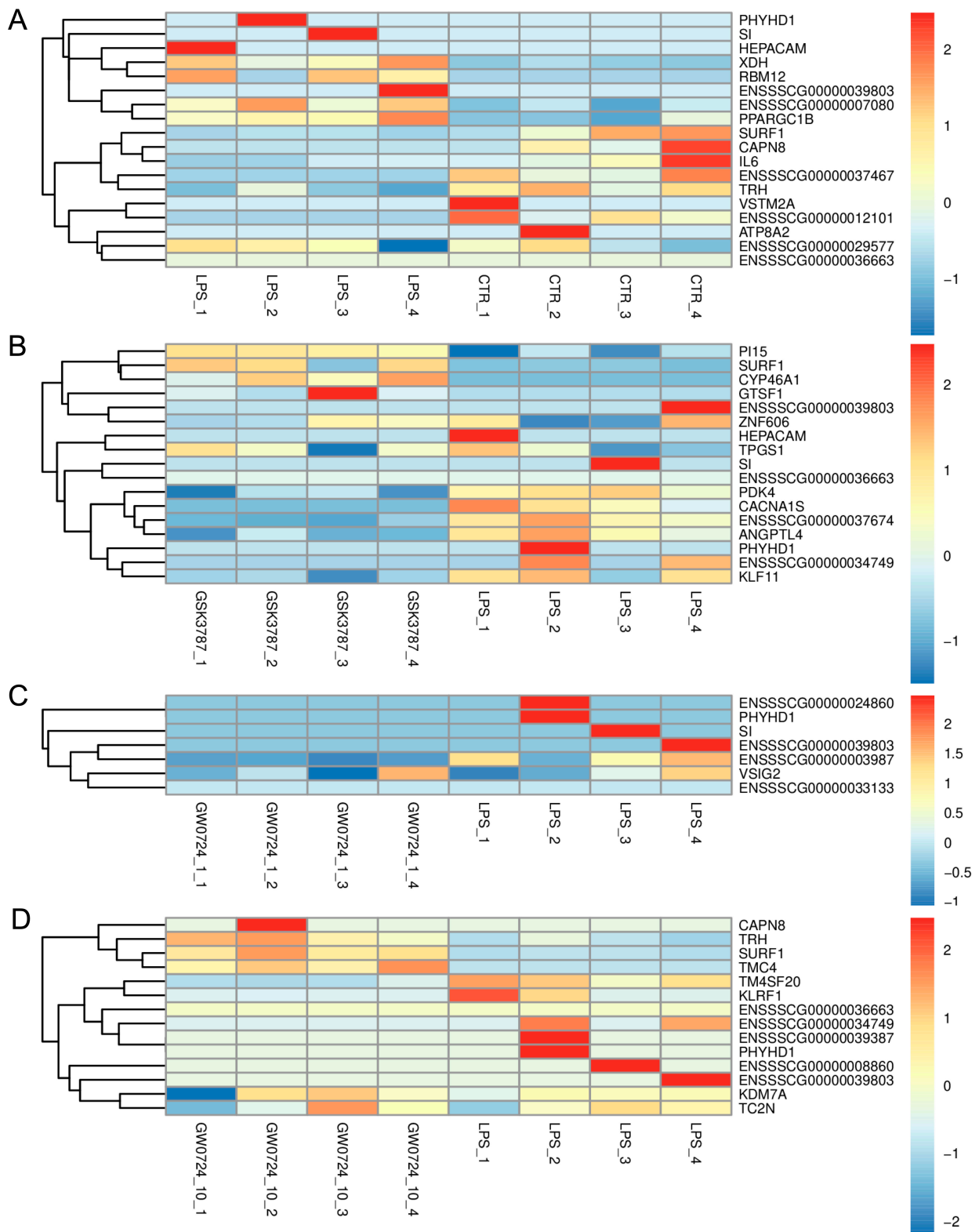


Figure 3. Hierarchical clustering heatmap of differentially expressed genes after LPS (A), GW0724 at a concentration of 1 $\mu\text{mol/L}$ (B), GW0724 at a concentration of 10 $\mu\text{mol/L}$ (C), or GSK3787 (D) treatment of porcine corpus luteum in the late-luteal phase of the estrous cycle.

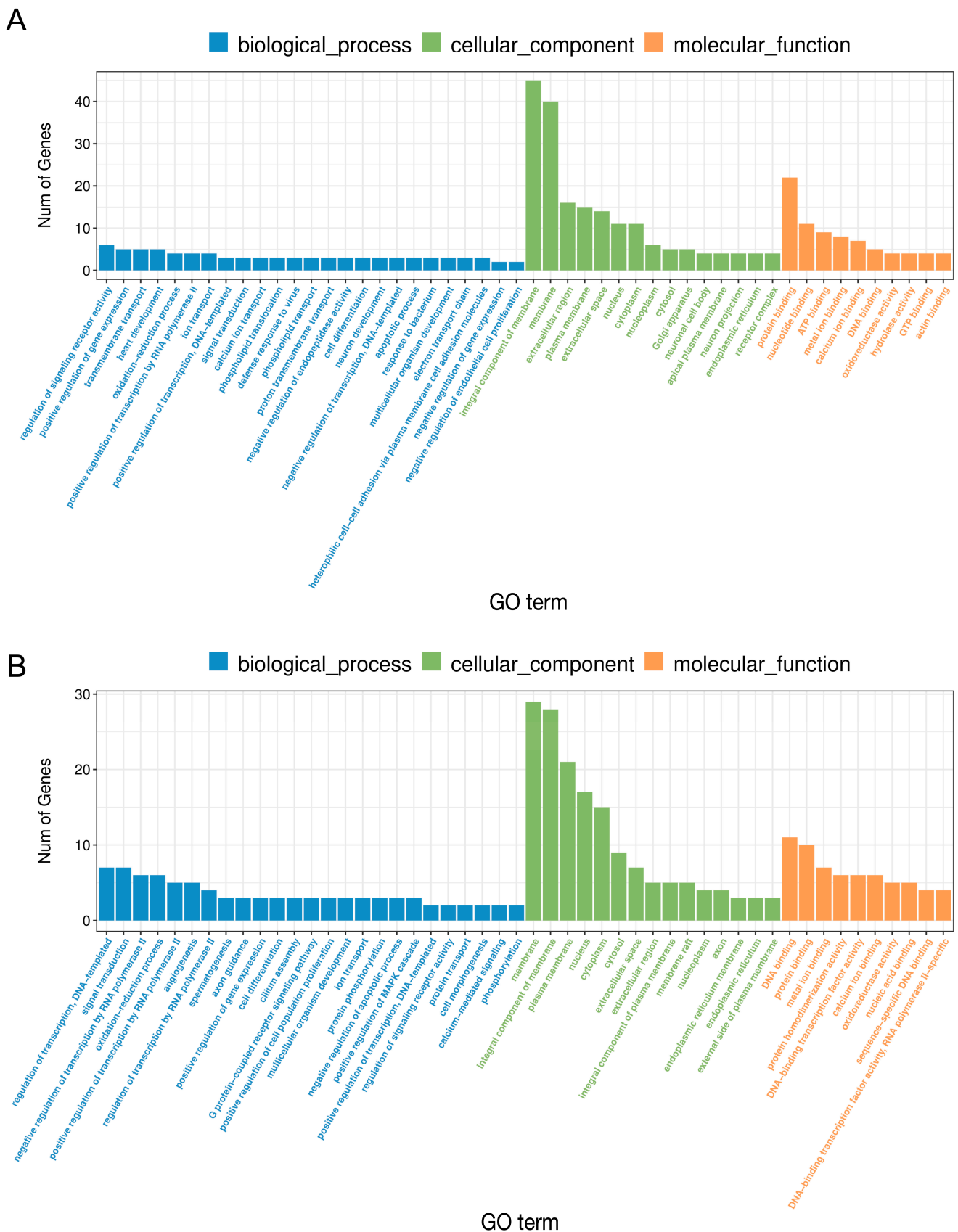


Figure 4. HierarchGO analysis of the differentially expressed genes after the treatment of the corpus luteum with LPS (A) or GW0724 at a concentration of 1 $\mu\text{mol/L}$ (B) in the mid-luteal phase of the estrous cycle. The x-axis indicates the terms of biological processes, while the y-axis indicates the number of significant enriched genes ($p < 0.05$).

2.3. The Effect of PPAR β/δ Agonist on Differential Gene Expression in the Corpus Luteum

The results of our study showed that the PPAR β/δ agonist GW0724 at a concentration of 1 $\mu\text{mol/L}$ affected the expression of 102 protein-coding genes (74 downregulated and 28 upregulated) (Figures 2B and 3B). The GO analysis assigned these DEGs to 193 terms of biological processes, 13 terms of cellular components, and 37 terms of molecular functions (Figure 4B). These DEGs were involved, for example, in oxidation–reduction processes (CYP46A1, CYP4A24, ALOX12B, ALDH3B2), immune response (IL-15, CSF3, TNFSF14, VTN) or cell population proliferation (SHH, MAB21L2, CSF3). Furthermore, KEEG analysis showed that these DEGs were engaged in pathways such as cytokine–cytokine receptor interaction (CD27, IL-15, CSF3, TNFSF14) or drug metabolism (TK1, ENSSSCG00000040980, ALDH3B2) (Supplemental Figure S1B). All detailed DEGs, GO and KEEG results were described in Supplemental Tables S6–S8 respectively.

In turn, the treatment of the CL with PPAR β/δ agonist GW0724 at a concentration of 10 $\mu\text{mol/L}$ resulted in changes in the expression of 103 genes (57 downregulated and 46 upregulated) (Figures 2C and 3C). The GO analysis assigned these DEGs to 275 terms of biological processes, 18 terms of cellular components, and 42 terms of molecular functions (Figure 5A). These DEGs were involved, for example, in immune and inflammatory response (LTA, CCL3L1, IL-6, TNFSF14, CCL4, ELF3), chemotaxis (PDGFRA, CCL3L1, ENSSSCG00000020934, CCL4), cellular response to lipopolysaccharide (CD180, IL-6, ZFP36) and tumor necrosis factor (CCL3L1, ZFP36, CCL4), or cytokine activity (LTA, CCL3L1, IL-6, TNFSF14, CCL4). Additionally, KEEG analysis indicated that these DEGs were engaged in pathways such as the NF-kappa B signaling pathway (LTA, TNFSF14, CCL4) or Toll-like receptor signaling pathway (LTA, CCL3L1, IL-6, CCL4) (Supplemental Figure S1C). All detailed DEGs, GO and KEEG results were described in Supplemental Tables S9–S11, respectively.

2.4. Comparative Analysis between Two Doses of PPAR β/δ Agonist

Statistical analysis identified 97 DEGs (19 downregulated and 78 upregulated) in the CL treated with GW0724 at a concentration of 10 $\mu\text{mol/L}$ compared with 1 $\mu\text{mol/L}$ (Supplemental Figure S2A, Supplemental Figure S2B). The GO analysis assigned these DEGs to 148 terms of biological processes, 8 terms of cellular components, and 32 terms of molecular functions (Supplemental Figure S2D). These DEGs were involved, for example, in immune and inflammatory response (ENSSSCG0000007642, CCL19, CSF3, MBL1, IL17B, CCR3), oxidation–reduction processes (CYP4A24, HSD17B3, SURF1) or response to DNA damage stimulus (MRNIP, BATF). Moreover, KEEG analysis indicated that these DEGs were engaged in pathways such as cytokine–cytokine receptor interaction (CCL19, IL17B, CSF3, CCR3, IL-27) and the IL-17 signaling pathway (IL17B, CSF3) (Supplemental Figure S2C). All detailed DEGs, GO and KEEG results were described in Supplemental Tables S12–S14, respectively.

2.5. The Effect of PPAR β/δ Antagonist on Differential Gene Expression in the Corpus Luteum

The study demonstrated that PPAR β/δ antagonist GSK3787 affected the expression of 88 protein-coding genes (63 downregulated and 25 upregulated) (Figures 2D and 3D). The GO analysis assigned these DEGs to 250 terms of biological processes, 16 terms of cellular components, and 39 terms of molecular functions (Figure 5B). These DEGs were mostly assigned to oxidation–reduction processes and oxidoreductase activity (CYP46A1, ENSSSCG0000003963, ALOX12B, ENOX1, CRYZL1, ENSSSCG00000030195) as well as angiogenesis (ANGPTL4, SHH, EPHB1, HAND1, LEP). Moreover, KEEG analysis indicated that these DEGs were engaged in pathways such as the PPAR signaling pathway (ANGPTL4, PLIN2) and cAMP signaling pathway (GRIN2B, GHRL, CACNA1S, PLN) (Supplemental Figure S1D). All detailed DEGs, GO and KEEG results were described in Supplemental Tables S15–S17, respectively.

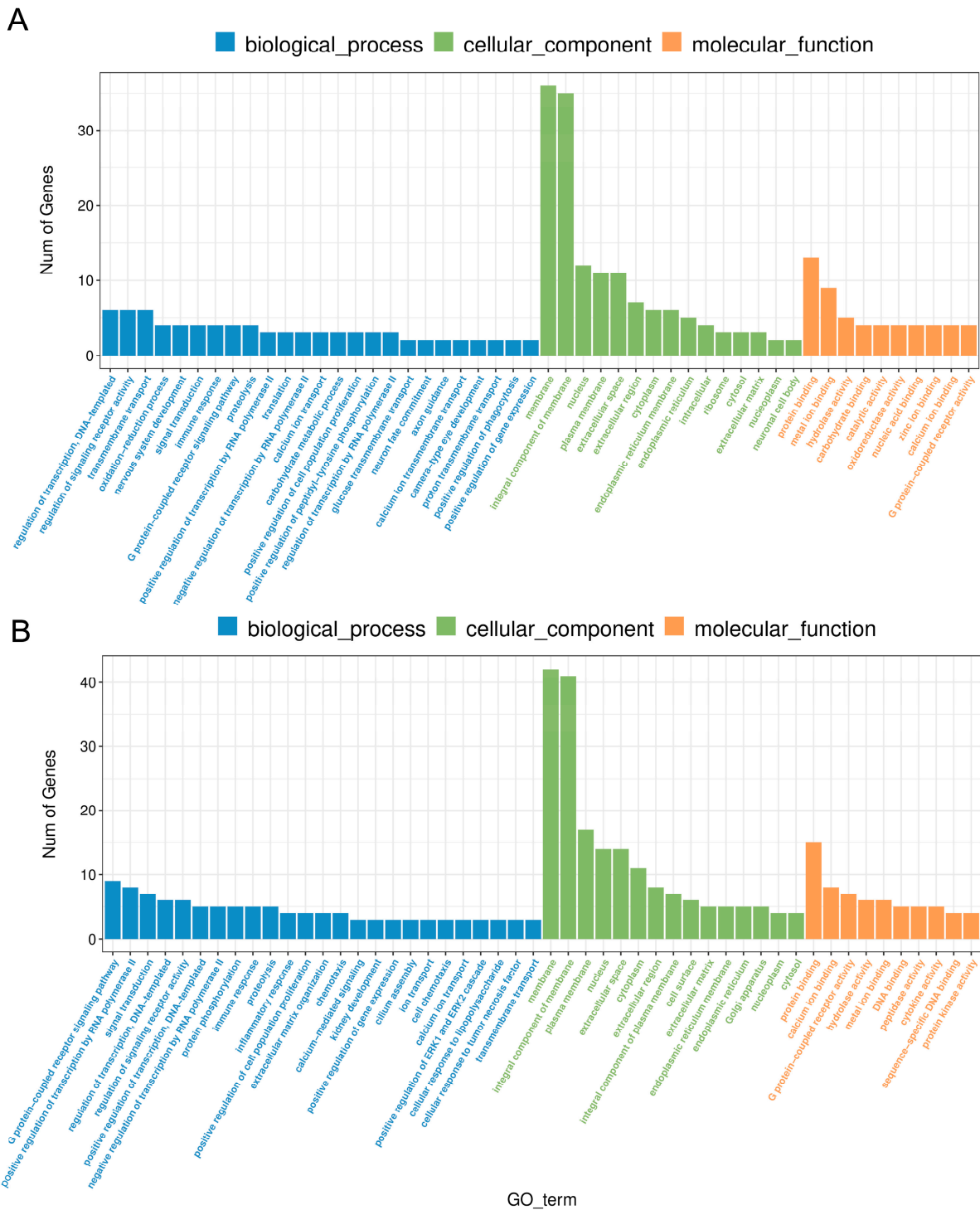


Figure 5. GO analysis of the differentially expressed genes after the treatment of the corpus luteum with GW0724 at a concentration of 10 $\mu\text{mol/L}$ (A) or GSK3787 (B) in the late-luteal phase of the estrous cycle. The x-axis indicates the terms of biological processes, while the y-axis indicates the number of significant enriched genes ($p < 0.05$).

2.6. Real-Time PCR Analysis

The treatment of the CL with LPS increased PPAR β/δ mRNA abundance during the mid-luteal phase of the estrous cycle (Supplemental Figure S3). Real-time PCR expression patterns of the tested DEGs (*IL-6*, *SOD2*, *CD180*, *ANGTPL4*) were in agreement with RNA-Seq results (Supplemental Figure S4).

2.7. Biochemical Analyses

Total antioxidant capacity was lower in the LPS-treated CL (21.66 mM Trolox/mg protein) compared with the control (33.97 mM Trolox/mg protein). Analysis of the CL, treated with PPAR β/δ agonist at a concentrations of 1 $\mu\text{mol/L}$ and 10 $\mu\text{mol/L}$, showed higher TAC levels compared with the LPS-treated CL. Moreover, TAC was enhanced with increasing agonist concentration (38.1 and 43.9 mM Trolox/mg protein, respectively). The total antioxidant capacity of the CL treated with the antagonist was similar to that of the CL treated with LPS (21.63 mM Trolox/mg protein) and no statistical difference was noted (Figure 6A).

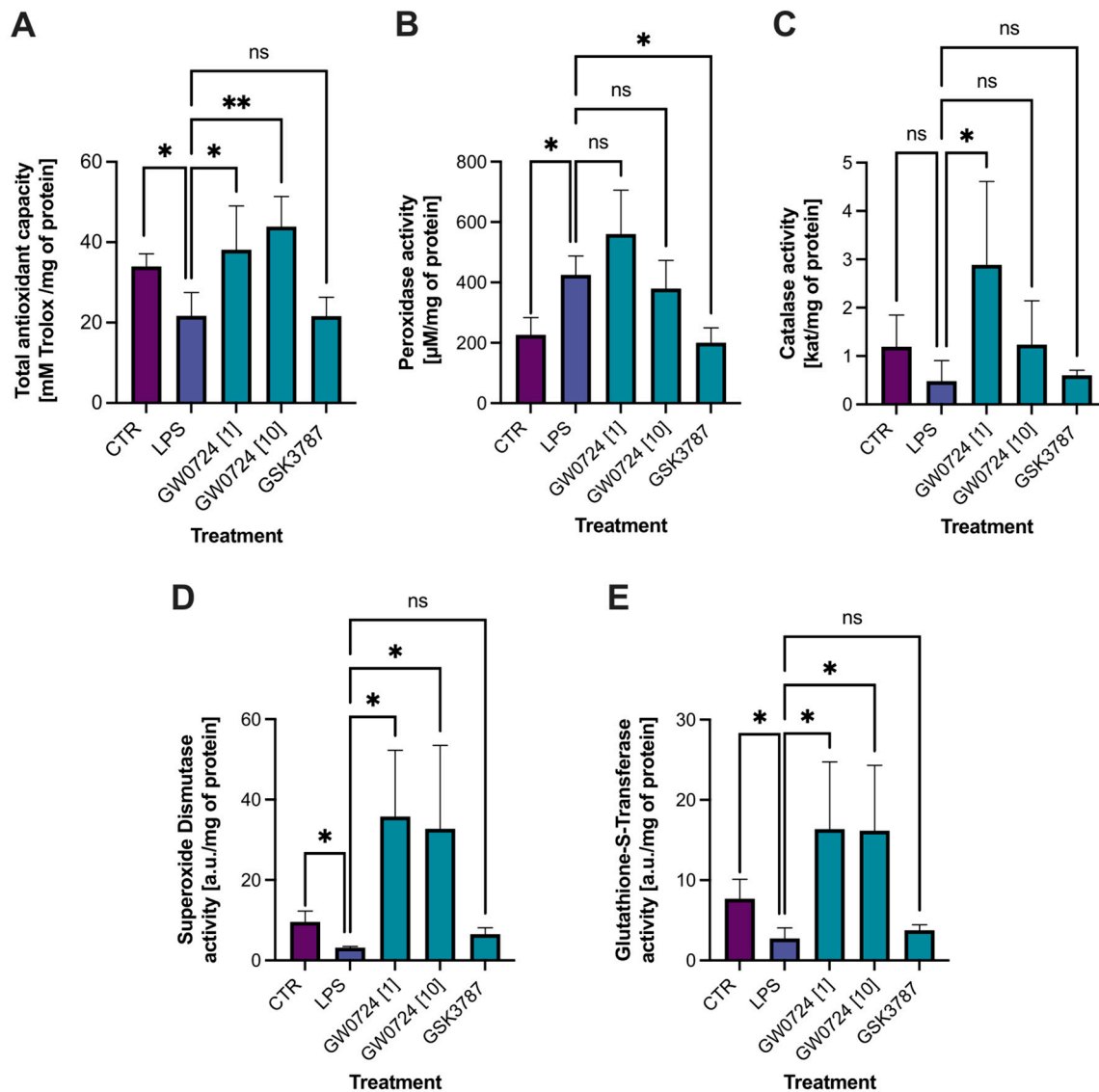


Figure 6. Different biochemical indicators of oxidative stress in corpus luteum treated with LPS or with LPS and PPAR β/δ agonist (GW0724 at a concentration of 1 $\mu\text{mol/L}$ or 10 $\mu\text{mol/L}$) and antagonist (GSK3787). Visualization of results of performed biochemical analyses: total antioxidant capacity (A), peroxidase activity (B), catalase activity (C), superoxide dismutase activity (D), glutathione-S-transferase activity (E). Results were considered statistically significant at $p \leq 0.05$ (*) and $p \leq 0.002$ (**); ns: not significant.

The activity of peroxidase in the CL increased almost 2-fold after stimulation with LPS compared with the control (226.4 vs. 424.8 $\mu\text{M}/\text{mg}$ protein). The difference in peroxidase activity in the agonist-treated CL compared with LPS-treated CL was not statistically significant. However, peroxidase activity in CL, which was treated with an antagonist

(200.2 $\mu\text{M}/\text{mg}$ protein), was decreased almost two-fold compared with LPS-treated CL (424.8 $\mu\text{M}/\text{mg}$ protein) (Figure 6B).

The activity of catalase in the CL did not change after LPS administration. Only the lower concentration of agonist compared with LPS-treated CL increased catalase activity (0.47 vs. 2.88 kat/mg protein) (Figure 6C).

The trend of the activity of SOD and GST was similar. The treatment of the CL with LPS decreased the activity of SOD almost three-fold compared with the control (9.58 vs. 3.18 a.u./mg protein). In turn, PPAR β/δ agonist GW0724 at concentrations of 1 $\mu\text{mol}/\text{L}$ or 10 $\mu\text{mol}/\text{L}$ increased the activity of SOD compared with the LPS-treated CL (1 $\mu\text{mol}/\text{L}$ –35.77 and 10 $\mu\text{mol}/\text{L}$ –32.72 a.u./mg protein) (Figure 6D). A similar observation was made with respect to GST activity. The treatment of the CL with LPS decreased the activity of GST compared with the control (7.69 vs. 2.74 a.u./mg protein), while the treatment with the agonist increased the activity of GST at both low and high concentrations (16.37 and 16.16 a.u./mg protein, respectively) compared with the LPS-treated CL. The activity of SOD or GST was not significantly affected by the PPAR β/δ antagonist (Figure 6E).

3. Discussion

A growing body of evidence shows a negative impact of lipopolysaccharide from *Escherichia coli* on reproductive functions. There are reports indicating that LPS leads to infertility by impairing ovarian functions [4]. It has been shown that LPS accumulates in follicular fluid, decreases the production of estradiol from granulosa cells, suppresses the expression of gonadotrophin receptors and disrupts blastocyst implantation [22]. Despite this evidence, transcriptome changes in the porcine corpus luteum under the influence of LPS had never been studied. The present results demonstrate for the first time the global transcriptomic profile of the CL of gilts during the mid-luteal phase of the estrous cycle and the effect of LPS as well as PPAR β/δ ligands during LPS-induced inflammation within the structure. We demonstrated that LPS affected the expression of 118 DEGs (63 of which were downregulated, whereas 55 were upregulated). These DEGs were assigned to different biological processes, such as response to bacterium, the negative regulation of endothelial cell proliferation, or the IL-17 signaling pathway.

Among the above genes with altered expression after LPS stimulation, we identified those involved in the regulation of oxidative stress and reactive oxygen species (ROS) production (*XDH*, *ALDH3B2*, *SOD2*, *ALOX12B*). It has been frequently reported that ROS play a significant and diverse role within the ovary, especially in the CL during luteal regression [23]. In addition, the abruptly increased production of ROS (e.g., by LPS during bacterial infection) decreases P₄ secretion, which may contribute to functional and structural luteolysis and disturb the proper course of the estrous cycle [24]. Xanthine dehydrogenase (*XDH*) is the rate-limiting enzyme for purine degradation, metabolizing hypoxanthine/xanthine to uric acid [25]. During these metabolic processes, numerous ROS are produced, including superoxide anion ($\text{O}_2^{\bullet-}$) and hydrogen peroxide (H_2O_2) [26]. In the present study, we demonstrated that *XDH* was upregulated in the LPS-treated CL during the mid-luteal phase of the estrous cycle. Moreover, we found that LPS downregulated the expression of *ALDH3B2* in the CL. This gene belongs to the aldehyde dehydrogenase (*ALDH*) family of enzymes, which is critical for the detoxification of aldehydes [27]. *ALDH3B1* has been reported to metabolize and protect cells from aldehydes and oxidative compounds derived from lipid peroxidation (LPO), suggesting an important role of this enzyme in cellular defense against oxidative stress and downstream aldehydes [28]. Mishra et al. [29] reported that the exposure of bovine luteal cells to LPS increased the LPO process. Based on our results, we can assume that LPS intensifies LPO and oxidative stress by increasing the expression of *XDH* and decreasing *ALDH3B2* in the porcine CL. Our studies revealed also that LPS increased the expression of *SOD2* in the CL during the mid-luteal phase of the estrous cycle. Superoxide dismutase 2 (*SOD2*) is known to play a crucial role as the major antioxidant defense system with increased expression under inflammatory conditions [30,31]. This enzyme efficiently converts superoxide to

the less reactive hydrogen peroxide (H_2O_2), which can diffuse out of mitochondria and be further detoxified to water by other antioxidant enzymes [32]. It has been reported that the antioxidant system (including SOD2) plays an important role in the maintenance of CL integrity and function during the estrous/menstrual cycle [33]. The luteal expression of *SOD2* appears to be dependent on the stage of the estrous cycle as well as the activity of various immune cells [24].

To confirm our transcriptomic results, we performed biochemical analyses to determine antioxidant status. We found that LPS reduced the total antioxidant capacity of the CL and decreased the activity of key antioxidant enzymes such as catalase, superoxide dismutase, and glutathione-s-transferase. It should be noted that *SOD2* gene expression was upregulated after LPS treatment, whereas superoxide dismutase activity decreased. The lack of correlation between mRNA and protein expression has been frequently described and is the result of differences in mRNA and protein stability and the differential regulation of post-transcriptional and translational processes [34–36].

An interesting part of our present research is the identification of genes involved in the immune response, such as *TNFSF14*, *NLRP6*, *IL-6* and *BMX*. Of particular interest seems to be *TNFSF14* (TNF Superfamily Member 14), which was upregulated in the CL after the treatment with LPS. *TNFSF14* is known to be a pro-inflammatory cytokine produced mainly by macrophages and T cells [37]. *TNFSF14* has been shown to promote the activation and maturation of T lymphocytes [38] and increase the production of ROS [39], which subsequently leads to severe inflammation and tissue destruction. In addition, *TNFSF14* has recently been proposed as one of the biomarkers for PCOS [40]. These results confirm that the use of LPS in the proposed experimental model induces an inflammatory response in porcine CL.

In the present studies, we investigated the effect of PPAR β/δ ligands on the CL treated with LPS under in vitro conditions. It is worth noting that stimulation with LPS increased the expression of PPAR β/δ , suggesting its regulatory role in inflamed tissue. Our experimental model included two concentrations of PPAR β/δ selective agonist (GW0724)—1 $\mu\text{mol/L}$ and 10 $\mu\text{mol/L}$. We found that 1 $\mu\text{mol/L}$ of GW0724 affected the expression of 102 DEGs (63 DEGs were downregulated and 39 DEGs were upregulated), whereas 10 $\mu\text{mol/L}$ of GW0724 altered the expression of 105 DEGs (58 DEGs were downregulated and 57 DEGs were upregulated). Most of these DEGs were involved in processes related to the regulation of oxidative stress and inflammation. Only the most interesting DEGs are discussed below.

In this study, we demonstrated that the activation of PPAR β/δ by GW0724 affected the expression of genes related to the control of oxidative stress, such as *ALDH3B2*, *SURF1*, *DUOXA2* and *PDK4*. The treatment of the LPS-stimulated CL with PPAR β/δ agonist at both doses decreased the expression of *ALDH3B2* (described earlier in the discussion) and *SURF1* (Surfeit locus protein 1), which is involved in the proper assembly of cytochrome c oxidase (COX) [41]. It is worth noting that these genes were upregulated after treatment with LPS alone, suggesting that activation of PPAR β/δ reverses the negative effect of LPS. Our study also showed the downregulation of *DUOXA2* (maturation factor of DOUX2) after treatment with GW0724 at a concentration of only 1 $\mu\text{mol/L}$. *DUOX2* is a membrane-localized glycoprotein composed of six transmembrane helices. In the presence of *DUOXA2*, these structural components regulate the transfer of electrons from NADPH to molecular oxygen to generate H_2O_2 [42]. *DUOXA2* expression has been reported to be increased during chronic inflammation and in various cancers, which may be related to the extensive production of ROS [43,44]. *DUOX2* upregulation has also been associated with a significant increase in extracellular H_2O_2 production and DNA damage in tissues [45]. In addition, it has been suggested that the pro-oxidant state resulting from the upregulation of *DUOX2* may impede the recovery of tissue damage caused by inflammatory stress [44]. Moreover, the current study also demonstrated that blocking PPAR β/δ by an antagonist upregulated *ENOX1* (Ecto-NOX disulfide thiol exchanger), a member of the ecto-NOX family involved in intracellular redox homeostasis [46]. *ENOX1* has been reported to induce oxidative

stress in human aortic endothelial cells [47]. Biochemical analyses determining antioxidant status confirmed the transcriptomic results. We demonstrated that the PPAR β/δ agonist reversed the LPS effect by increasing the activity of superoxide dismutase, glutathione transferase and catalase. The obtained results suggest that the use of the PPAR β/δ agonist attenuates oxidative stress and prevents tissue damage. Conversely, blocking the receptor may increase oxidative stress.

The present study has revealed the regulatory role of GW0724, a PPAR β/δ agonist, in the inflammatory process in the porcine CL. Interestingly, the observed effects appear to be dependent on the dose of ligand administered. The treatment with GW0724 at a concentration of 1 $\mu\text{mol/L}$ revealed six DEGs (*CSF3*, *VTN*, *IL-15*, *C1QTNF12*, *DUOX2*, *TNFSF14*) involved in the regulation of the inflammatory response or immune processes, according to the Gene Ontology analysis. In this work, we have demonstrated the inhibitory effect of GW0724 on the expression of *CSF3* (Granulocyte colony-stimulating factor 3), the major regulator of neutrophil production [48]. *CSF3* has been reported to exert pro-inflammatory properties in inflammatory joint diseases. There is also evidence that a deficiency of *CSF3* protects mice from acute and chronic arthritis [48]. An inhibitory effect of GW0724 on the expression of a potent proinflammatory cytokine—*TNFSF14*—was also observed. It is worth noting that this is the opposite effect to that observed after LPS treatment alone.

The current results showed that GW0724 (1 $\mu\text{mol/L}$) decreased the expression of *VTN* (Vitronectin), a pro-inflammatory glycoprotein that binds to integrin receptors [49]. *VNT*-deficient mice were found to have lower numbers of neutrophils and lower concentrations of pro-inflammatory cytokines such as *IL-1 β* and *IL-6* in the lungs after LPS exposure than *VTN*-positive mice [50]. Moreover, the exposure of mice to *VTN* was associated with the decreased apoptosis of neutrophils [51]. In addition to its anti-apoptotic effect, *VTN* may also exacerbate the severity of acute lung injury by decreasing the uptake and clearance of apoptotic neutrophils by alveolar and tissue-derived macrophages, which is associated with the release of pro-inflammatory mediators [52].

The treatment with GW0724 (1 $\mu\text{mol/L}$) upregulated the expression of *IL-15* in inflamed CL. Interleukin 15 is a pleiotropic cytokine involved in the inflammatory response in various infectious diseases [53]. It has been reported that *IL-15* plays an important role in host defense in sepsis induced in mice by *E. coli* [54]. Mice overexpressing *IL-15* were resistant to the septic shock induced by *E. coli*, which was related to the inhibition of apoptosis triggered by *TNF- α* . Moreover, the treatment of normal mice with exogenous *IL-15* made them resistant to *E. coli*-induced lethal shock [54].

The treatment of inflamed CL with GW0724 at a concentration of 10 $\mu\text{mol/L}$ affected the expression of eight genes involved in the regulation of inflammatory responses or immune processes (*CD180*, *IL-6*, *CCL3L1*, *LT α* , *CCL4*, *ELF3*, *ZFP36*, *TNFSF14*). In contrast to the lower dose of GW0724 (1 $\mu\text{mol/L}$), which showed an anti-inflammatory character, the higher dose (10 $\mu\text{mol/L}$) seems to be pro-inflammatory. We have shown that the expression of *CD180*, a specific inhibitor of TLR4-mediated inflammatory response [55], was downregulated after the treatment of inflamed CL with GW0724 at the higher dose. *CD180* is an accessory TLR4 molecule expressed in various cell types, including monocytes and macrophages [30]. In addition, we detected the increased expression of *IL-6*, *CCL3L1*, *CCL4*, *LT α* and *ELF3*, which are genes known to possess pro-inflammatory properties, mainly expressed through the induction of chemotaxis and the activation of lymphocytes and macrophages [56–59].

Statistical analysis performed between the two PPAR β/δ agonist doses revealed 19 downregulated and 77 upregulated genes. The most interesting genes are involved in the regulation of inflammatory and immune responses. Among them are *MBL1*, *CCL19*, *IL-17 β* , *PGLYRP3* and *CSF3*, whose expression was higher after treatment with GW0724 at a concentration of 10 $\mu\text{mol/L}$ compared with 1 $\mu\text{mol/L}$. Mannan-binding lectin (MBL) is an important factor of innate immunity that contributes to the elimination of microorganisms. MBL has been reported to bind to bacteria and then neutralize them by opsonizing and activating complement through the lectin pathway of complement activation [60].

In turn, peptidoglycan recognition protein 3 (PGLYRP3) recognizes bacterial compounds (peptidoglycan) and plays a role in antibacterial innate immunity [61]. Both factors are crucial during the first step of bacterial infection. The chemokine CCL19 triggers T cell proliferation, leading to upregulation of pro-inflammatory cytokine synthesis [62]. It has been reported that IL-17B induces monocytes to produce TNF- α and IL-1 β and supports neutrophil recruitment and B cell chemotaxis [63,64]. During infection, immune cells such as granulocytes, macrophages, and lymphocytes are recruited to tissues to clear bacterial infection [6]. We propose that PPAR β/δ may not only play a key role in alleviating chronic inflammation, but may also be helpful in supporting the immune response to bacterial infection in the CL.

4. Materials and Methods

4.1. Experimental Animals

The study was conducted on corpora lutea harvested from gilts intended for commercial slaughter and meat processing in accordance with the guidelines for animal care (the Act of 15 January 2015 on the Protection of Animals Used for Scientific or Educational Purposes and Directive 2010/63/EU of the European Parliament and the Council of 22 September 2010 on the protection of animals used for scientific purposes). Experimental material was collected from adult crossbred gilts (Large White \times Polish Landrace, 7 months old, 100 kg body weight, $n = 4$) on days 10–12 of the estrous cycle (mid-luteal phase). On the farm, pigs were observed in two consecutive heat cycles. The first mark of estrus (the behavior of gilts observed in the presence of the boar) was defined as day 0 of the estrous cycle. The animals were transported to the local slaughterhouse where the ovaries were dissected within a few minutes. The removed tissues were transferred to the laboratory on ice in phosphate-buffered saline (PBS) with an antibiotic cocktail (100 IU/mL penicillin and 100 mg/mL streptomycin, PolfaTarchomin, Poland). The phase of the estrous cycle was proven in the laboratory from the morphological characteristics of the ovary [65].

4.2. In Vitro Experiment

The procedure for collection and incubation of the porcine CL was previously described [66]. In the laboratory, the CL were dissected from the ovary, connective tissue was removed, and placed on ice in a sterile Petri dish. CLs were cut into small pieces (100 ± 10 mg, in duplicate from each experimental replicate). Each tissue explant was placed in M199 medium (Sigma Aldrich, St. Louis, MO, USA) supplemented with 0.1% BSA fraction V (Roth, Germany) and antibiotics. The explants were pre-incubated for 2 h in a water bath at 37 °C in an atmosphere of 95% O₂ and 5% CO₂. Then, the explants were treated with LPS (100 ng/mL, from *E. coli*) for 24 h. Explants not treated with LPS were considered as controls. The medium was removed, and the explants were incubated for 6 h with LPS alone or in combination with the PPAR β/δ ligands: GW0724 (agonist; 1 μ mol/L or 10 μ mol/L, Cayman Chemical Company, Ann Arbor, MI, USA) or GSK3787 (antagonist; 25 μ mol/L, Cayman Chemical Company). Controls also contained dimethyl sulfoxide (DMSO, solvent for the tested PPAR ligands). After the incubation, tissue explants were frozen at -80 °C until further analysis.

4.3. RNA Isolation, Library Preparation and Sequencing Procedure

Total RNA from 20 samples was isolated using the “RNeasy Mini Kit” (Qiagen, Hilden, Germany) according to the manufacturer’s protocol. The Tecan Infinite M200 plate reader (Tecan Group Ltd., Männedorf, Switzerland) and Agilent Bioanalyzer 2100 (Agilent Technology, Santa Clara, CA, USA) were used to evaluate total RNA quantity and quality. The samples with an RNA Integrity Number (RIN) of >7 were selected for the next analyses. The poly(A) RNA-sequencing library was prepared according to the Illumina TruSeq Stranded mRNA Sample Preparation Protocol. Two rounds of purification were performed using oligo(dT) magnetic beads to purify the poly(A) tailed mRNA. Subsequently, the poly(A) RNA was fragmented at high temperature using a divalent cation buffer, and

poly(dT) oligonucleotides were used to transcribe the RNA into cDNA. Subsequently, the cDNA was subjected to 3' tail adenylation and adapter ligation. Reverse transcription during library construction was strand-specific. Finally, the libraries were pooled and then sequenced. Quality control analysis and quantification of the sequencing libraries were performed using the Agilent Technologies 2100 Bioanalyzer High Sensitivity DNA Chip. Paired-end sequencing was performed using the Illumina NovaSeq 6000 Sequencing System (LC Science, Houston, TX, USA).

4.4. Transcript Assembly and Analysis of Differentially Expressed Genes

FastQC was used to assess sequence quality. After removing low-quality reads, the remaining 150 bp paired-end sequences were reassembled and mapped to the *Sus scrofa* genome using HISAT2 [67,68]. The mapped reads from each sample were assembled using StringTie [68]. All transcriptomes were then merged to reconstruct a comprehensive transcriptome using Perl scripts and GffCompare. Once the final transcriptome was constructed, StringTie and edgeR [69] were used to estimate the expression levels of all transcripts. StringTie was used to determine the expression of mRNAs by calculating fragments per kilobase of transcript per million (FPKM) [68]. Differentially expressed genes (DEGs) were selected with \log_2 (fold change) > 1 or \log_2 (fold change) < -1 and with statistical significance (p -value < 0.05) using the R package edgeR [69].

4.5. Real-Time PCR

Differentially expressed genes were validated via real-time PCR using the AriaMx real-time PCR System (Agilent Technology, Santa Clara, CA, USA), as previously described [70]. Primer sequences (Supplemental Table S1) for reference and target genes (*IL-6*, *SOD2*, *CD180*, *ANGTPL4*, *PPAR β/δ*) were designed via Primer Express Software 3 (Applied Biosystems, Waltham, MA, USA). The abundance of the tested mRNAs was calculated using the comparative Pfaffl method [71]. The constitutively expressed *ACTB* and *GAPDH* genes were implemented as reference genes, and the geometric mean values of the expression levels were used for analysis. Real-time PCR results were analyzed using Statistica software (version 13.1; Statsoft Inc. Tulsa, OK, USA) with Student's t test and expressed as means \pm SEM. Results were considered statistically significant at $p \leq 0.05$.

4.6. Biochemical Analyses

4.6.1. Tissue Extract Preparation for Biochemical Analyses

The extract of the CL tissue after in vitro culture for biochemical analyses (in 5 technical replicates of each sample) was prepared via mechanical homogenization (Omni tissue Homogenizer, Kennesaw, GA, USA) in sterile PBS. Extracts were centrifuged ($5000 \times g$) at 4 °C for 15 min, and the supernatant was transferred to new tubes containing 500 μ L. Protein concentration was determined using the bicinchoninic acid method (Pierce BCA Protein Assay Kit, Thermo Fisher Scientific, Waltham, MA, USA) according to the manufacturer's protocol.

4.6.2. Antioxidant Capacity

Total antioxidant capacity (TAC) was analyzed using the improved ABTS radical cation decolorization assay according to Re et al. [72]. The pre-formed radical monocation of 2,2'-azinobis-(3-ethylbenzothiazoline-6-sulfonic acid) (ABTS^{•+}) was generated via the oxidation of ABTS with potassium persulfate and was reduced in the presence of such hydrogen-donating antioxidants. The results were calculated as Trolox (a water-soluble analogue of vitamin E) equivalents per L per mg of protein.

4.6.3. Peroxidase Activity

Peroxidase activity was determined according to the method described by Chance and Maehly [73]. The method consists of determining the content of purpurogallin, an orange crystalline compound in the incubation mixture, formed when pyrogallol is oxidized as a hydrogen donor in the presence of hydrogen peroxide. Samples were mixed with

pyrogallol and hydrogen peroxide and incubated at 30 °C for 4 min. Absorbance was measured at 430 nm against air. The difference between the absorbance of the control sample (0.05 M acetate buffer at pH 5.6 was added instead of the tissue homogenate) and the tested sample (tissue homogenate) was a measure of enzyme activity. The millimolar absorbance coefficient for purpurogallin was 2.47/mM·cm. Enzyme activity was converted to mg of protein in the assay.

4.6.4. Catalase Activity

The measurement method is based on the ability of catalase to decompose hydrogen peroxide [74]. The reaction is accompanied by a decrease in absorbance at a wavelength of 240 nm. Briefly, samples were diluted 20 times with 0.2 M phosphate buffer at pH 7. A total of 100 µL of H₂O₂ was then added to 200 µL of the sample. The absorbance was measured relative to the control (buffer instead of sample) for 30 s at 5 s intervals. The value of the decrease in absorbance was determined and the activity expressed in katal per mg of protein.

4.6.5. Superoxide Dismutase Activity

The method for determining the activity of superoxide dismutase (SOD) uses the ability of p-iodonitrotetrazolium [2-(4-iodophenyl)-3-(4-nitrophenyl)-5-phenyltetrazolium; INT] to be reduced to a water-soluble product with an absorption maximum at about 505 nm (reddish pink) by superoxide anion (O²⁻), which is formed during the oxidation reaction of xanthine by xanthine oxidase [74]. The rate of reduction of INT is linearly related to the activity of xanthine oxidase and is inhibited by SOD. Superoxide dismutase inhibits the reduction of INT to purple formazan by scavenging this radical. The rate of formazan formation is a measure of the activity of SOD [75]. The activity of SOD was expressed in arbitrary units [a. u.] per mg of protein.

4.6.6. Glutathione S-Transferase Activity

The glutathione S-transferase (GST) activity was determined using the Rice-Evans [76] method. Enzyme activity was calculated based on the millimolar absorption coefficient (9.6 mmol⁻¹/cm⁻¹) for the glutathione conjugate formed from 1-chloro-2,4-dinitrobenzene. The GST activity was converted to arbitrary units [a. u.] per mg of protein.

4.6.7. Statistical Analysis for Biochemical Analyses

Statistical analysis for the obtained results was performed using *t*-test in Prism 9 software (version 9.1.1 (223); GraphPad Software Inc., San Diego, CA, USA). Results were considered statistically significant at $p \leq 0.05$ (*) and $p \leq 0.002$ (**).

5. Conclusions

In conclusion, this is the first report describing the *in vitro* effects of different doses of PPAR β/δ agonist (GW0742) on LPS-induced inflammation in the CL. We imply that PPAR β/δ ligands act in two ways depending on the dose. We have shown that both doses of the ligand exert a positive effect on the oxidative status during inflammation. Moreover, we postulate that lower dose of GW0724 effectively inhibits the expression of potent pro-inflammatory mediators, whereas the higher dose increases the expression of pro-inflammatory factors, which are mostly responsible for the induction of chemotaxis and the functional and proliferative activation of leukocytes. Therefore, we propose that the lower dose of GW0724 can be used to alleviate chronic inflammation, while the higher dose can be used to support the natural anti-pathogen response during the acute phase of inflammation that occurs at the onset of bacterial infection.

Supplementary Materials: The following supporting information can be downloaded at: <https://www.mdpi.com/article/10.3390/ijms24054993/s1>.

Author Contributions: Conceptualization: K.M. and I.B.; methodology: K.M.; software: K.M.; validation: K.M.; formal analysis: K.M., A.K. and R.S.; investigation: Z.G., K.M., A.K., M.G. and R.S.; resources: K.M. and I.B.; data curation: K.M.; writing—original draft preparation: K.M.; writing—review and editing: I.B.; visualization, K.M.; supervision: I.B.; project administration: K.M.; funding acquisition: K.M. All authors have read and agreed to the published version of the manuscript.

Funding: This research was supported by the National Science Centre of Poland, Grant No. 2019/35/N/NZ9/01706.

Institutional Review Board Statement: The study was conducted according to the Polish Act of the protection of animals used for educational or scientific purposes of 15 January 2015 and directive 2010/63/EU (Journal of Laws Dz.U. 2015 No. item 266) of the European Parliament of 22 September 2010 (2010/63/EU) on the protection of animals used for scientific objectives, so this study did not require the consent of a competent ethics committee for animal experiments.

Informed Consent Statement: Not applicable.

Data Availability Statement: The datasets generated and/or analyzed during the current study are available in the ArrayExpress database; Accession: E-MTAB-12027 <https://www.ebi.ac.uk/biostudies/arrayexpress/studies/E-MTAB-12027> (accessed on 1 September 2022).

Acknowledgments: We would like to thank Elżbieta Łopieńska-Biernat for assistance with biochemical analysis.

Conflicts of Interest: The authors declare no conflict of interest.

References

1. Schmid-Schönbein, G.W. Analysis of Inflammation. *Annu. Rev. Biomed. Eng.* **2006**, *8*, 93–151. [[CrossRef](#)] [[PubMed](#)]
2. Herath, S.; Fischer, D.P.; Werling, D.; Williams, E.J.; Lilly, S.T.; Dobson, H.; Bryant, C.E.; Sheldon, I.M. Expression and Function of Toll-Like Receptor 4 in the Endometrial Cells of the Uterus. *Endocrinology* **2006**, *147*, 562–570. [[CrossRef](#)] [[PubMed](#)]
3. Cronin, J.G.; Turner, M.L.; Goetze, L.; Bryant, C.E.; Sheldon, I.M. Toll-Like Receptor 4 and MYD88-Dependent Signaling Mechanisms of the Innate Immune System Are Essential for the Response to Lipopolysaccharide by Epithelial and Stromal Cells of the Bovine Endometrium1. *Biol. Reprod.* **2012**, *86*, 51. [[CrossRef](#)] [[PubMed](#)]
4. Lavon, Y.; Leitner, G.; Goshen, T.; Braw-Tal, R.; Jacoby, S.; Wolfenson, D. Exposure to Endotoxin during Estrus Alters the Timing of Ovulation and Hormonal Concentrations in Cows. *Theriogenology* **2008**, *70*, 956–967. [[CrossRef](#)] [[PubMed](#)]
5. Lüttgenau, J.; Herzog, K.; Strüve, K.; Latter, S.; Boos, A.; Bruckmaier, R.M.; Bollwein, H.; Kowalewski, M.P. LPS-Mediated Effects and Spatio-Temporal Expression of TLR2 and TLR4 in the Bovine Corpus Luteum. *Reproduction* **2016**, *151*, 391–399. [[CrossRef](#)] [[PubMed](#)]
6. Williams, E.J.; Herath, S.; England, G.C.W.; Dobson, H.; Bryant, C.E.; Sheldon, I.M. Effect of Escherichia Coli Infection of the Bovine Uterus from the Whole Animal to the Cell. *Animal* **2008**, *2*, 1153–1157. [[CrossRef](#)]
7. Daniel, J.A.; Abrams, M.S.; DeSouza, L.; Wagner, C.G.; Whitlock, B.K.; Sartin, J.L. Endotoxin Inhibition of Luteinizing Hormone in Sheep. *Domest. Anim. Endocrinol.* **2003**, *25*, 13–19. [[CrossRef](#)]
8. Herzog, K.; Strüve, K.; Kastelic, J.P.; Piechotta, M.; Ulbrich, S.E.; Pfarrer, C.; Shirasuna, K.; Shimizu, T.; Miyamoto, A.; Bollwein, H. Escherichia Coli Lipopolysaccharide Administration Transiently Suppresses Luteal Structure and Function in Diestrous Cows. *Reproduction* **2012**, *144*, 467–476. [[CrossRef](#)]
9. Meurens, F.; Summerfield, A.; Nauwynck, H.; Saif, L.; Gerds, V. The Pig: A Model for Human Infectious Diseases. *Trends Microbiol.* **2012**, *20*, 50–57. [[CrossRef](#)]
10. Takada, I.; Makishima, M. Peroxisome Proliferator-Activated Receptor Agonists and Antagonists: A Patent Review (2014-Present). *Expert Opin. Pat.* **2020**, *30*, 1–13. [[CrossRef](#)] [[PubMed](#)]
11. Zerani, M.; Polisca, A.; Boiti, C.; Maranesi, M. Current Knowledge on the Multifactorial Regulation of Corpora Lutea Lifespan: The Rabbit Model. *Animals* **2021**, *11*, 296. [[CrossRef](#)] [[PubMed](#)]
12. Parillo, F.; Maranesi, M.; Brecchia, G.; Gobbetti, A.; Boiti, C.; Zerani, M. In Vivo Chronic and In Vitro Acute Effects of Di(2-Ethylhexyl) Phthalate on Pseudopregnant Rabbit Corpora Lutea: Possible Involvement of Peroxisome Proliferator-Activated Receptor Gamma1. *Biol. Reprod.* **2014**, *90*, 41. [[CrossRef](#)]
13. Zerani, M.; Maranesi, M.; Brecchia, G.; Gobbetti, A.; Boiti, C.; Parillo, F. Evidence for a Luteotropic Role of Peroxisome Proliferator-Activated Receptor Gamma: Expression and In Vitro Effects on Enzymatic and Hormonal Activities in Corpora Lutea of Pseudopregnant Rabbits1. *Biol. Reprod.* **2013**, *88*, 62. [[CrossRef](#)]
14. Clark, R.B. The Role of PPARs in Inflammation and Immunity. *J. Leukoc. Biol.* **2002**, *71*, 388–400. [[CrossRef](#)]
15. Mierzejewski, K.; Paukszto, Ł.; Kurzyńska, A.; Kunicka, Z.; Jastrzębski, J.P.; Makowczenko, K.G.; Golubska, M.; Bogacka, I. PPARγ Regulates the Expression of Genes Involved in the DNA Damage Response in an Inflamed Endometrium. *Sci. Rep.* **2022**, *12*, 4026. [[CrossRef](#)]

16. Mierzejewski, K.; Kurzyńska, A.; Kunicka, Z.; Klepacka, A.; Golubska, M.; Bogacka, I. Peroxisome Proliferator-Activated Receptor Gamma Ligands Regulate the Expression of Inflammatory Mediators in Porcine Endometrium during LPS-Induced Inflammation. *Theriogenology* **2022**, *187*, 195–204. [[CrossRef](#)]
17. Liu, Y.; Colby, J.; Zuo, X.; Jaoude, J.; Wei, D.; Shureiqi, I. The Role of PPAR- δ in Metabolism, Inflammation, and Cancer: Many Characters of a Critical Transcription Factor. *Int. J. Mol. Sci.* **2018**, *19*, 3339. [[CrossRef](#)]
18. Dunn, S.E.; Bhat, R.; Straus, D.S.; Sobel, R.A.; Axtell, R.; Johnson, A.; Nguyen, K.; Mukundan, L.; Moshkova, M.; Dugas, J.C.; et al. Peroxisome Proliferator-Activated Receptor δ Limits the Expansion of Pathogenic Th Cells during Central Nervous System Autoimmunity. *J. Exp. Med.* **2010**, *207*, 1599–1608. [[CrossRef](#)] [[PubMed](#)]
19. Connelly, T.L.; Baer, S.E.; Cooper, J.T.; Bronk, D.A.; Wawrik, B.; Harding, K.; Turk-Kubo, K.A.; Sipler, R.E.; Mills, M.M.; Bronk, D.A.; et al. Printing from Here Is Disabled. *Deep Sea Res. 2 Top. Stud. Ocean.* **2019**, *118*, 1–13. [[CrossRef](#)]
20. Matsushita, Y.; Ogawa, D.; Wada, J.; Yamamoto, N.; Shikata, K.; Sato, C.; Tachibana, H.; Toyota, N.; Makino, H. Activation of Peroxisome Proliferator-Activated Receptor δ Inhibits Streptozotocin-Induced Diabetic Nephropathy Through Anti-Inflammatory Mechanisms in Mice. *Diabetes* **2011**, *60*, 960–968. [[CrossRef](#)]
21. Luz-Crawford, P.; Ipseiz, N.; Espinosa-Carrasco, G.; Caicedo, A.; Tejedor, G.; Toupet, K.; Loriau, J.; Scholtyssek, C.; Stoll, C.; Khoury, M.; et al. PPAR β/δ Directs the Therapeutic Potential of Mesenchymal Stem Cells in Arthritis. *Ann. Rheum. Dis.* **2016**, *75*, 2166–2174. [[CrossRef](#)] [[PubMed](#)]
22. Li, H.; Guo, S.; Cai, L.; Ma, W.; Shi, Z. Lipopolysaccharide and Heat Stress Impair the Estradiol Biosynthesis in Granulosa Cells via Increase of HSP70 and Inhibition of Smad3 Phosphorylation and Nuclear Translocation. *Cell Signal.* **2017**, *30*, 130–141. [[CrossRef](#)] [[PubMed](#)]
23. Moravek, M.B.; Ward, E.A.; Lebovic, D.I. Thiazolidinediones as Therapy for Endometriosis: A Case Series. *Gynecol. Obs. Invest.* **2009**, *68*, 167–170. [[CrossRef](#)] [[PubMed](#)]
24. Talukder, S.; Kerrisk, K.L.; Gabai, G.; Celi, P. Role of Oxidant–Antioxidant Balance in Reproduction of Domestic Animals. *Anim. Prod. Sci.* **2017**, *57*, 1588. [[CrossRef](#)]
25. Okamoto, K.; Kusano, T.; Nishino, T. Chemical Nature and Reaction Mechanisms of the Molybdenum Cofactor of Xanthine Oxidoreductase. *Curr. Pharm. Des.* **2013**, *19*, 2606–2614. [[CrossRef](#)] [[PubMed](#)]
26. Battelli, M.G.; Polito, L.; Bortolotti, M.; Bolognesi, A. Xanthine Oxidoreductase-Derived Reactive Species: Physiological and Pathological Effects. *Oxid. Med. Cell Longev.* **2016**, *2016*, 3527579. [[CrossRef](#)]
27. Brichac, J.; Ho, K.K.; Honzatko, A.; Wang, R.; Lu, X.; Weiner, H.; Picklo, M.J. Enantioselective Oxidation of Trans -4-Hydroxy-2-Nonenal Is Aldehyde Dehydrogenase Isozyme and Mg²⁺ Dependent. *Chem. Res. Toxicol.* **2007**, *20*, 887–895. [[CrossRef](#)] [[PubMed](#)]
28. Marchitti, S.A.; Bocker, C.; Orlicky, D.J.; Vasiliou, V. Molecular Characterization, Expression Analysis, and Role of ALDH3B1 in the Cellular Protection against Oxidative Stress. *Free Radic. Biol. Med.* **2010**, *49*, 1432–1443. [[CrossRef](#)]
29. Mishra, D.P.; Dhali, A. Endotoxin Induces Luteal Cell Apoptosis through the Mitochondrial Pathway. *Prostaglandins Other Lipid. Mediat.* **2007**, *83*, 75–88. [[CrossRef](#)]
30. Yoon, S.; Hong, M.; Wilson, I.A. An Unusual Dimeric Structure and Assembly for TLR4 Regulator RP105–MD-1. *Nat. Struct. Mol. Biol.* **2011**, *18*, 1028–1035. [[CrossRef](#)]
31. Yi, L.; Shen, H.; Zhao, M.; Shao, P.; Liu, C.; Cui, J.; Wang, J.; Wang, C.; Guo, N.; Kang, L.; et al. Inflammation-Mediated SOD-2 Upregulation Contributes to Epithelial-Mesenchymal Transition and Migration of Tumor Cells in Aflatoxin G1-Induced Lung Adenocarcinoma. *Sci. Rep.* **2017**, *7*, 7953. [[CrossRef](#)]
32. Flynn, J.M.; Melov, S. SOD2 in Mitochondrial Dysfunction and Neurodegeneration. *Free Radic. Biol. Med.* **2013**, *62*, 4–12. [[CrossRef](#)] [[PubMed](#)]
33. Al-Gubory, K.H.; Garrel, C.; Faure, P.; Sugino, N. Roles of Antioxidant Enzymes in Corpus Luteum Rescue from Reactive Oxygen Species-Induced Oxidative Stress. *Reprod. Biomed. Online* **2012**, *25*, 551–560. [[CrossRef](#)] [[PubMed](#)]
34. Schwanhäusser, B.; Wolf, J.; Selbach, M.; Busse, D. Synthesis and Degradation Jointly Determine the Responsiveness of the Cellular Proteome. *BioEssays* **2013**, *35*, 597–601. [[CrossRef](#)]
35. Gry, M.; Rimini, R.; Strömberg, S.; Asplund, A.; Pontén, F.; Uhlén, M.; Nilsson, P. Correlations between RNA and Protein Expression Profiles in 23 Human Cell Lines. *BMC Genom.* **2009**, *10*, 365. [[CrossRef](#)] [[PubMed](#)]
36. Schwanhäusser, B.; Busse, D.; Li, N.; Dittmar, G.; Schuchhardt, J.; Wolf, J.; Chen, W.; Selbach, M. Global Quantification of Mammalian Gene Expression Control. *Nature* **2011**, *473*, 337–342. [[CrossRef](#)]
37. Kim, W.-J.; Kang, Y.-J.; Koh, E.-M.; Ahn, K.-S.; Cha, H.-S.; Lee, W.-H. LIGHT Is Involved in the Pathogenesis of Rheumatoid Arthritis by Inducing the Expression of Pro-Inflammatory Cytokines and MMP-9 in Macrophages. *Immunology* **2005**, *114*, 272–279. [[CrossRef](#)]
38. Shaikh, R.B.; Santee, S.; Granger, S.W.; Butrovich, K.; Cheung, T.; Kronenberg, M.; Cheroutre, H.; Ware, C.F. Constitutive Expression of LIGHT on T Cells Leads to Lymphocyte Activation, Inflammation, and Tissue Destruction. *J. Immunol.* **2001**, *167*, 6330–6337. [[CrossRef](#)]
39. Otterdal, K.; Haukeland, J.W.; Yndestad, A.; Dahl, T.B.; Holm, S.; Segers, F.M.; Gladhaug, I.P.; Konopski, Z.; Damås, J.K.; Halvorsen, B.; et al. Increased Serum Levels of LIGHT/TNFSF14 in Nonalcoholic Fatty Liver Disease: Possible Role in Hepatic Inflammation. *Clin. Transl. Gastroenterol.* **2015**, *6*, e95. [[CrossRef](#)]

40. Hatziagelaki, E.; Pergialiotis, V.; Kannenberg, J.M.; Trakakis, E.; Tsiavou, A.; Markgraf, D.F.; Carstensen-Kirberg, M.; Pacini, G.; Roden, M.; Dimitriadis, G.; et al. Association between Biomarkers of Low-Grade Inflammation and Sex Hormones in Women with Polycystic Ovary Syndrome. *Exp. Clin. Endocrinol. Diabetes* **2020**, *128*, 723–730. [[CrossRef](#)]
41. Tiranti, V.; Hoertnagel, K.; Carrozzo, R.; Galimberti, C.; Munaro, M.; Granatiero, M.; Zelante, L.; Gasparini, P.; Marzella, R.; Rocchi, M.; et al. Mutations of SURF-1 in Leigh Disease Associated with Cytochrome c Oxidase Deficiency. *Am. J. Hum. Genet.* **1998**, *63*, 1609–1621. [[CrossRef](#)]
42. De Deken, X.; Corvilain, B.; Dumont, J.E.; Miot, F. Roles of DUOX-Mediated Hydrogen Peroxide in Metabolism, Host Defense, and Signaling. *Antioxid. Redox. Signal.* **2014**, *20*, 2776–2793. [[CrossRef](#)] [[PubMed](#)]
43. Lipinski, S.; Till, A.; Sina, C.; Arlt, A.; Grasberger, H.; Schreiber, S.; Rosenstiel, P. DUOX2-Derived Reactive Oxygen Species Are Effectors of NOD2-Mediated Antibacterial Responses. *J. Cell. Sci.* **2009**, *122*, 3522–3530. [[CrossRef](#)]
44. Wu, Y.; Antony, S.; Meitzler, J.L.; Doroshov, J.H. Molecular Mechanisms Underlying Chronic Inflammation-Associated Cancers. *Cancer Lett.* **2014**, *345*, 164–173. [[CrossRef](#)] [[PubMed](#)]
45. Chen, C.; Zhou, Y.; Hu, C.; Wang, Y.; Yan, Z.; Li, Z.; Wu, R. Mitochondria and Oxidative Stress in Ovarian Endometriosis. *Free Radic. Biol. Med.* **2019**, *136*, 22–34. [[CrossRef](#)] [[PubMed](#)]
46. Scarlett, D.-J.G.; Herst, P.M.; Berridge, M.V. Multiple Proteins with Single Activities or a Single Protein with Multiple Activities: The Conundrum of Cell Surface NADH Oxidoreductases. *Biochim. Et. Biophys. Acta BBA-Bioenerg.* **2005**, *1708*, 108–119. [[CrossRef](#)] [[PubMed](#)]
47. Lee, S.; Li, R.; Kim, B.; Palvolgyi, R.; Ho, T.; Yang, Q.-Z.; Xu, J.; Szeto, W.L.; Honda, H.; Berliner, J.A. Ox-PAPC Activation of PMET System Increases Expression of Heme Oxygenase-1 in Human Aortic Endothelial Cell. *J. Lipid. Res.* **2009**, *50*, 265–274. [[CrossRef](#)]
48. Lawlor, K.E.; Campbell, I.K.; Metcalf, D.; O'Donnell, K.; van Nieuwenhuijze, A.; Roberts, A.W.; Wicks, I.P. Critical Role for Granulocyte Colony-Stimulating Factor in Inflammatory Arthritis. *Proc. Natl. Acad. Sci. USA* **2004**, *101*, 11398–11403. [[CrossRef](#)]
49. Welser-Alves, J.V.; Milner, R. Microglia Are the Major Source of TNF- α and TGF-B1 in Postnatal Glial Cultures; Regulation by Cytokines, Lipopolysaccharide, and Vitronectin. *Neurochem. Int.* **2013**, *63*, 47–53. [[CrossRef](#)]
50. Tsuruta, Y.; Park, Y.-J.; Siegal, G.P.; Liu, G.; Abraham, E. Involvement of Vitronectin in Lipopolysaccharide-Induced Acute Lung Injury. *J. Immunol.* **2007**, *179*, 7079–7086. [[CrossRef](#)]
51. Bae, H.-B.; Zmijewski, J.W.; Deshane, J.S.; Zhi, D.; Thompson, L.C.; Peterson, C.B.; Chaplin, D.D.; Abraham, E. Vitronectin Inhibits Neutrophil Apoptosis through Activation of Integrin-Associated Signaling Pathways. *Am. J. Respir. Cell. Mol. Biol.* **2012**, *46*, 790–796. [[CrossRef](#)]
52. Park, Y.-J.; Liu, G.; Lorne, E.F.; Zhao, X.; Wang, J.; Tsuruta, Y.; Zmijewski, J.; Abraham, E. PAI-1 Inhibits Neutrophil Efferocytosis. *Proc. Natl. Acad. Sci. USA* **2008**, *105*, 11784–11789. [[CrossRef](#)]
53. Budagian, V.; Bulanova, E.; Paus, R.; Bulfonepaus, S. IL-15/IL-15 Receptor Biology: A Guided Tour through an Expanding Universe. *Cytokine Growth Factor Rev.* **2006**, *17*, 259–280. [[CrossRef](#)]
54. Hiromatsu, T.; Yajima, T.; Matsuguchi, T.; Nishimura, H.; Wajjwalku, W.; Arai, T.; Nimura, Y.; Yoshikai, Y. Overexpression of Interleukin-15 Protects against Escherichia Coli –Induced Shock Accompanied by Inhibition of Tumor Necrosis Factor- α –Induced Apoptosis. *J. Infect. Dis.* **2003**, *187*, 1442–1451. [[CrossRef](#)] [[PubMed](#)]
55. Divanovic, S.; Trompette, A.; Atabani, S.F.; Madan, R.; Golenbock, D.T.; Visintin, A.; Finberg, R.W.; Tarakhovskiy, A.; Vogel, S.N.; Belkaid, Y.; et al. Negative Regulation of Toll-like Receptor 4 Signaling by the Toll-like Receptor Homolog RP105. *Nat. Immunol.* **2005**, *6*, 571–578. [[CrossRef](#)] [[PubMed](#)]
56. Kaplanski, G. IL-6: A Regulator of the Transition from Neutrophil to Monocyte Recruitment during Inflammation. *Trends Immunol.* **2003**, *24*, 25–29. [[CrossRef](#)]
57. Kouno, J.; Nagai, H.; Nagahata, T.; Onda, M.; Yamaguchi, H.; Adachi, K.; Takahashi, H.; Teramoto, A.; Emi, M. Up-Regulation of CC Chemokine, CCL3L1, and Receptors, CCR3, CCR5 in Human Glioblastoma That Promotes Cell Growth. *J. Neurooncol.* **2004**, *70*, 301–307. [[CrossRef](#)]
58. Calmon-Hamaty, F.; Combe, B.; Hahne, M.; Morel, J. Lymphotoxin α Revisited: General Features and Implications in Rheumatoid Arthritis. *Arthritis Res.* **2011**, *13*, 232. [[CrossRef](#)]
59. Suzuki, M.; Saito-Adachi, M.; Arai, Y.; Fujiwara, Y.; Takai, E.; Shibata, S.; Seki, M.; Rokutan, H.; Maeda, D.; Horie, M.; et al. E74-Like Factor 3 Is a Key Regulator of Epithelial Integrity and Immune Response Genes in Biliary Tract Cancer. *Cancer Res.* **2021**, *81*, 489–500. [[CrossRef](#)] [[PubMed](#)]
60. Kilpatrick, D.C. Mannan-Binding Lectin and Its Role in Innate Immunity. *Transfus. Med.* **2002**, *12*, 335–352. [[CrossRef](#)] [[PubMed](#)]
61. Royet, J.; Dziarski, R. Peptidoglycan Recognition Proteins: Pleiotropic Sensors and Effectors of Antimicrobial Defences. *Nat. Rev. Microbiol.* **2007**, *5*, 264–277. [[CrossRef](#)] [[PubMed](#)]
62. Marsland, B.J.; Bättig, P.; Bauer, M.; Ruedl, C.; Lässig, U.; Beerli, R.R.; Dietmeier, K.; Ivanova, L.; Pfister, T.; Vogt, L.; et al. CCL19 and CCL21 Induce a Potent Proinflammatory Differentiation Program in Licensed Dendritic Cells. *Immunity* **2005**, *22*, 493–505. [[CrossRef](#)] [[PubMed](#)]
63. Li, H.; Chen, J.; Huang, A.; Stinson, J.; Heldens, S.; Foster, J.; Dowd, P.; Gurney, A.L.; Wood, W.I. Cloning and Characterization of IL-17B and IL-17C, Two New Members of the IL-17 Cytokine Family. *Proc. Natl. Acad. Sci. USA* **2000**, *97*, 773–778. [[CrossRef](#)]
64. Shi, Y.; Ullrich, S.J.; Zhang, J.; Connolly, K.; Grzegorzewski, K.J.; Barber, M.C.; Wang, W.; Wathen, K.; Hodge, V.; Fisher, C.L.; et al. A Novel Cytokine Receptor-Ligand Pair. *J. Biol. Chem.* **2000**, *275*, 19167–19176. [[CrossRef](#)] [[PubMed](#)]
65. Akins, E.L.; Morrissette, M.C. Gross Ovarian Changes during Estrous Cycle of Swine. *Am. J. Vet. Res.* **1968**, *29*, 1953–1957.

66. Kunicka, Z.; Mierzejewski, K.; Kurzyńska, A.; Stryński, R.; Mateos, J.; Carrera, M.; Bogacka, I. Analysis of Changes in the Proteomic Profile of Porcine Corpus Luteum during Different Stages of the Estrous Cycle: Effects of PPAR Gamma Ligands. *Reprod. Fertil. Dev.* **2022**, *34*, 776–788. [[CrossRef](#)]
67. Martin, M. Cutadapt Removes Adapter Sequences from High-Throughput Sequencing Reads. *EMBnet J.* **2011**, *17*, 10. [[CrossRef](#)]
68. Kim, D.; Langmead, B.; Salzberg, S.L. HISAT: A Fast Spliced Aligner with Low Memory Requirements. *Nat. Methods* **2015**, *12*, 357–360. [[CrossRef](#)]
69. Robinson, M.D.; McCarthy, D.J.; Smyth, G.K. EdgeR: A Bioconductor Package for Differential Expression Analysis of Digital Gene Expression Data. *Bioinformatics* **2010**, *26*, 139–140. [[CrossRef](#)]
70. Mierzejewski, K.; Paukzsto, Ł.; Kurzyńska, A.; Kunicka, Z.; Jastrzębski, J.P.; Bogacka, I. Transcriptome Analysis of Porcine Endometrium after LPS-Induced Inflammation: Effects of the PPAR-Gamma Ligands in Vitro. *Biol. Reprod.* **2021**, *104*, 130–143. [[CrossRef](#)]
71. Pfaffl, M.W. A New Mathematical Model for Relative Quantification in Real-Time RT-PCR. *Nucleic. Acids Res.* **2001**, *29*, e45. [[CrossRef](#)] [[PubMed](#)]
72. Re, R.; Pellegrini, N.; Proteggente, A.; Pannala, A.; Yang, M.; Rice-Evans, C. Antioxidant Activity Applying an Improved ABTS Radical Cation Decolorization Assay. *Free Radic. Biol. Med.* **1999**, *26*, 1231–1237. [[CrossRef](#)] [[PubMed](#)]
73. Chance, B.; Maehly, A.C. [136] Assay of catalases and peroxidases. In *Methods in Enzymology*; Elsevier Inc.: Amsterdam, The Netherlands, 1955; Volume 2, pp. 764–775. [[CrossRef](#)]
74. Aebi, H. [13] Catalase in Vitro. In *Methods in Enzymology*; Elsevier Inc.: Amsterdam, The Netherlands, 1984; Volume 104, pp. 121–126. [[CrossRef](#)]
75. Podcasy, J.J.; Wei, R. Reduction of Iodonitrotetrazolium Violet by Superoxide Radicals. *Biochem Biophys Res. Commun.* **1988**, *150*, 1294–1301. [[CrossRef](#)] [[PubMed](#)]
76. Rice-Evans, C.; Miller, N.J. [241] Total antioxidant status in plasma and body fluids. In *Methods in Enzymology*; Elsevier Inc.: Amsterdam, The Netherlands, 1994; Volume 234, pp. 279–293. [[CrossRef](#)]

Disclaimer/Publisher’s Note: The statements, opinions and data contained in all publications are solely those of the individual author(s) and contributor(s) and not of MDPI and/or the editor(s). MDPI and/or the editor(s) disclaim responsibility for any injury to people or property resulting from any ideas, methods, instructions or products referred to in the content.